Research Article | Vol. 30, No. 15 / 18 Jul 2022 / Optics Express 27602
Optics EXPRESS

Waveguide structure based electron acceleration using terahertz pulses

SZABOLCS TURNÁR,[1] GERGŐ KRIZSÁN,[1,2] JÁNOS HEBLING,[1,2,3] AND ZOLTÁN TIBAI[1,*]

[1] *Institute of Physics, University of Pécs, 7624 Pécs, Hungary*
[2] *Szentágothai Research Centre, University of Pécs, 7624 Pécs, Hungary*
[3] *ELKH-PTE High-Field Terahertz Research Group, 7624 Pécs, Hungary*
[*] *tibai@fizika.ttk.pte.hu*

Abstract: We have developed a waveguide structure for electron acceleration using a few μJ energy THz pulse. The metallic device focuses the incoming linearly polarized nearly single-cycle THz pulse, hence increasing the peak electric field strength. We experimentally verified the gain and the temporal profile of the electric field in the structure using electro-optic sampling technique. The acceleration of the electron bunch from rest up to 8 keV was predicted using single-cycle THz pulses with μJ-energy level.

1. Introduction

Conventional particle accelerator technology has been developed continuously over the past century, however the limited acceleration field and the used low frequency (<10 GHz) requires hundreds of meter long facilities to achieve the demanded energies. By looking for alternative and more compact solutions, novel acceleration concepts, such as laser plasma acceleration [1,2], laser-driven dielectric acceleration [3,4] and terahertz (THz) driven acceleration [5,6] were demonstrated for electron beam acceleration, each with different advantages and disadvantages.

In the recent years due to the appearance of new THz generation techniques, μJ and even mJ-level THz sources were demonstrated [7–10], paving the way to the THz-based particle acceleration and manipulation. The efficient THz-driven particle acceleration requires electric field strength of MV/cm, which is still quite challenging despite the promising THz generation techniques. Tight focusing of the THz pulses can be a solution, however, the diffraction limited focusing alone does not provide the appropriate conditions for efficient particle acceleration. Looking for alternative solutions, waveguide structures seem to be promising and make it possible to reduce the beam waist to be less than a wavelength and to produce MV/cm peak electric field strength even applying only μJ energy level THz pulses.

In this paper we introduce an optimized waveguide structure-based electron accelerator setup powered by THz pulse with μJ energy level. Using a horn-shaped metallic waveguide structure we focused the incoming linearly polarized nearly single-cycle THz pulse below the diffraction limit, thereby increasing the peak electric field strength. We experimentally verified the gain and the temporal profile of the electric field in the horn-gun structure using electro-optic sampling technique and by numerical simulations we proved that the horn-gun is applicable for electron acceleration.

2. Waveguide structure-based electron acceleration

Nowadays, the THz-driven waveguide-structure based particle acceleration and manipulation is a very active, and continuously emerging research area. The development of the different types of waveguides gives a chance to both compress and stabilize the relativistic electron bunches [11–13] and manipulate ultrafast electron bunches [14–16]. Further possibilities, such as to

#459282 https://doi.org/10.1364/OE.459282
Journal © 2022 Received 29 Mar 2022; revised 22 May 2022; accepted 24 May 2022; published 14 Jul 2022

Optics EXPRESS

accelerate the bunch as an electron gun [17,18], to post-accelerate the bunch [19–23] or measure the length of the electron bunches by the effect of streaking [24,25] are also available.

The waveguide with two parallel horn-couplers is called horn-gun. Our horn-gun based experimental setup is illustrated in Fig. 1(b). In the setup, the THz pulse is focused to the input surface of the horn-gun using an off-axis parabolic mirror. The horn-gun consists of two main parts: the tapered horn part and the rectangular waveguide channel. While the THz pulse propagates through the tapered part, its peak electric field increases significantly. In the waveguide channel the THz pulse propagates further, while the electrons are emitted from one side wall. The beam size of the THz pulse is much smaller than the wavelength and the peak electric field strength is in the MV/cm level at the interaction zone, so by synchronizing the generation time of the electrons, effective acceleration can be achieved. After the interaction between the electrons and the accelerating part of the THz field, the electrons can propagate through the pinhole, which was fabricated on the other (opposite to the electron emitter) side of the channel. The important and necessary condition to operate the device as an electron gun is that the accelerated electrons must leave the channel before the decelerating half of the THz pulse reaches the interaction zone. Minimization of the effect of the decelerating part can be achieved by optimizing the dimensions of the waveguide channel and/or the peak electric field of the THz pulse. By closing the end of the horn-gun, the peak electric field strength at the acceleration zone can be further increased due to the interference of the forward propagating and reflected pulses, thereby more efficient acceleration can be achieved.

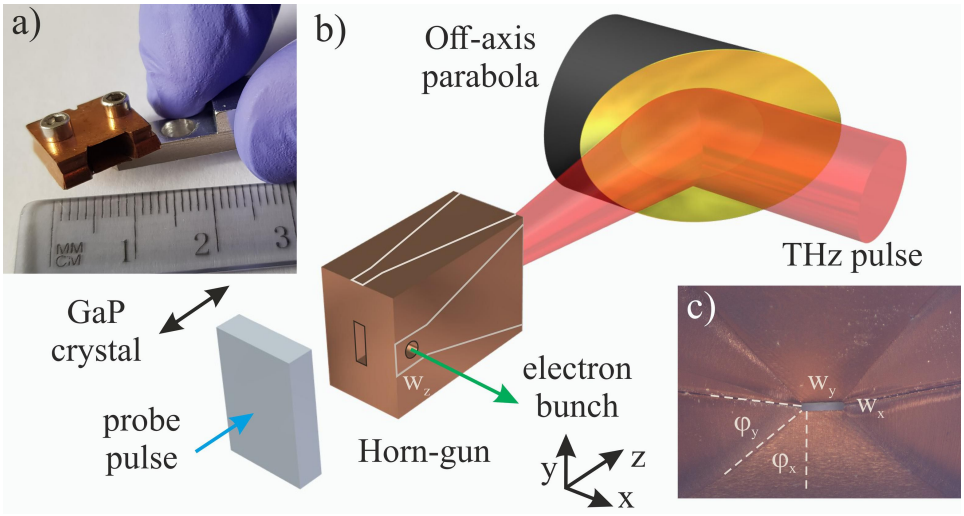

Fig. 1. (a) Horn-gun based electron gun. (b) Schematic view of the experiment. (c) Inside view of the horn-gun (image was taken by Sergey Antipov).

In our study both the tapered horn structure and the channel part were optimized. The evaluation of the THz-field propagation through the device was accomplished by electromagnetic field simulations using the CST Studio Suite software [26]. The achievable peak electric field in the channel significantly depends on the length and on the φ_x and φ_y angles (see Fig. 1(c)) of the horn-coupler in x and y planes, respectively. According to our calculations the highest peak electric field was obtained for $\varphi_x = 16°$ and $\varphi_y = 10°$, and the peak electric field strength has increased by around a factor of 15 compared to the initial peak electric field at the entrance plane. It means that using optimized focusing of the THz pulse having a few μJ energy, the electric field strength has exceeded the MV/cm level in the interaction region. The material of the horn-gun is copper. In order to avoid the damage of the material the peak electric field strength cannot

Optics EXPRESS

exceed 8 MV/cm [27]. In our measurement the central frequency of the THz pulse was 0.55 THz (see chapter 3). An important aspect concerning the parameters of the channel was the cut off frequency and the requirement that the acceleration has to be realized efficiently with rest electrons. Considering the frequency of the THz pulse, for the sizes of the rectangular channel $w_x = 50$ μm and $w_y = 400$ μm were chosen. The length of the channel (w_z) is 300 μm, which is fixed to λ/2 as a condition for constructive interference.

The manufactured horn-gun is shown in Fig. 1(a). It is only 11 mm long and the sizes of the input opening are 3.6 and 6.1 mm in the x- and y (transversal) directions, respectively. The inside view of the waveguide is shown in Fig. 1(c).

3. THz pulse characterization using EO sampling

The horn-shaped metallic waveguide structure was tested by removing the end of the device in order to make possible the outcoupling of THz pulse from the device after propagating through it. A GaP crystal was attached to the back of the metallic waveguide structure to measure the waveform of the transmitted THz pulse by reflective EO sampling technique. The complete arrangement is shown in Fig. 2. The THz pulse was generated by a tilted-pulse-front excitation scheme [28]. The central wavelength of the pump was 1030 nm and its pulse duration was 200 fs. The nonlinear material was a 6 mol% MgO doped congruent lithium-niobate. The groove density of the grating was 1400 1/mm. For the imaging cylindrical lenses were used ($L1 = 250$ mm, $L2 = 150$ mm). The source, which was detected by a calibrated pyroelectric detector (SLT THz 20), was optimized for THz energy. The THz waveform was detected by electro-optic sampling in a 1.2 mm thick sandwiched GaP crystal. The thickness of the active layer (with 110 orientation), which faced the horn-gun, was 0.2 mm. The field-induced birefringence acting on the probe beam was detected by a combination of a λ/4 plate, a Wollaston-prism, and a pair of balanced photodiodes. The temporal evolution of the terahertz electric field was sampled by the variation of the time delays between the pump and probe pulses. The THz spot size was detected by a pyroelectric camera (Pyrocam IV).

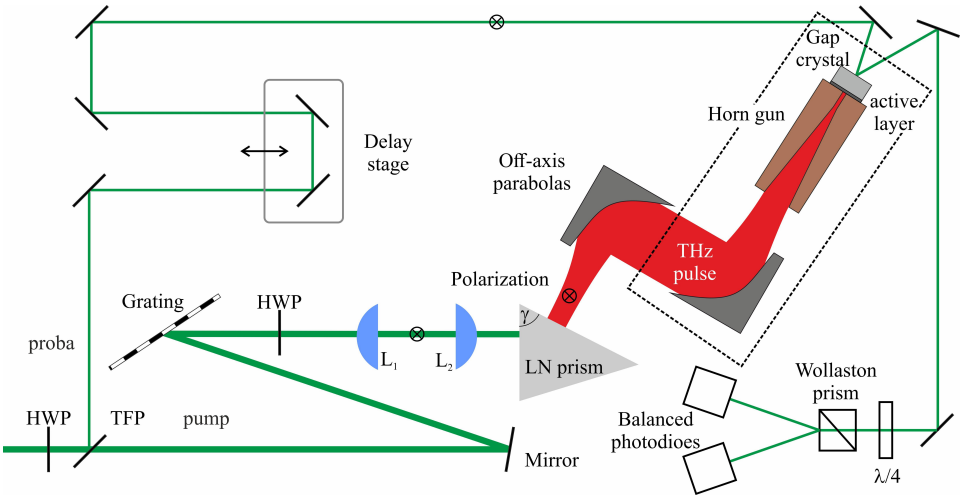

Fig. 2. Schematic view of THz pulse generation and electro-optic sampling setup.

The experimentally measured and numerically simulated pulse shapes at different positions are shown in Figs. 3(a)-(c). Figure 3(a) shows the experimentally measured temporal shape of the THz pulse at the input surface of the horn-gun. This measured temporal shape was imported to the CST software to follow the evaluation of the THz pulse inside the horn-gun device and

Optics EXPRESS

simulate the particle acceleration in the waveguide part. At the entrance plane the THz beam diameter was 3.18 mm x 2.82 mm ($1/e^2$) and the energy was 0.98 μJ. The peak electric field was 114 kV/cm, which was calculated (similarly to [8]) from the measured spot size, energy and the measured temporal shape of the electric field. Figure 3(b) shows the temporal profile of the THz pulse at the electron injection point, i.e., at the half distance of the waveguide channel in the z direction. Due to the dispersion, at the electron injection point the number of the cycles is increased, while the electric field strength is also increased by about a factor of 10 compared to the electric field at the entrance plane. Figure 3(c) shows the temporal shapes of the measured (by reflective EO sampling) and simulated (by CST) THz pulses at the end of the device (at the exit plane), respectively. The two temporal shapes show a good agreement. At the end of the device the peak electric field was calculated from the w_x x w_y horn-gun dimensions, the outcoupled energy (~0.2 μJ) and the measured temporal shape of the electric field. It was 777 kV/cm, that is 7 times larger than the initial peak electric field.

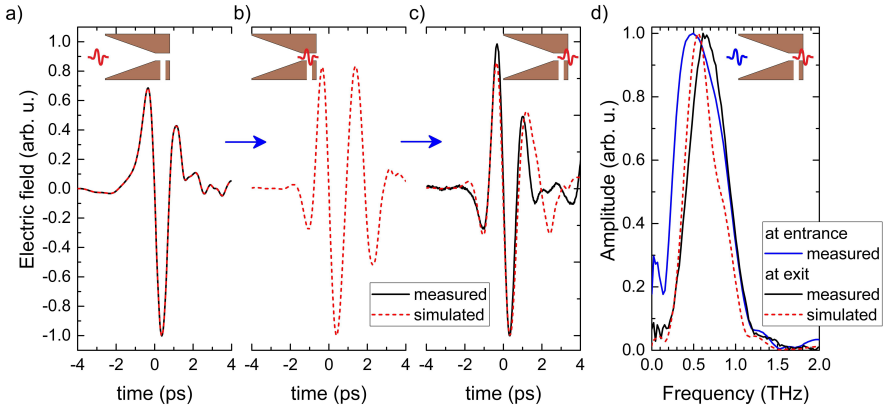

Fig. 3. (a) Electric field of the THz pulse at the entrance of the horn-gun, (b) at the injection point of the electron, (c) and at the exit of the horn-gun channel. (d) Spectra of the pulses at the entrance and at the exit of the horn-gun.

Figure 3(d) shows the spectra of the experimentally measured and simulated pulses at the entrance plane and at the end of the horn-gun as well. In case of the experimental and simulated results, the attenuation of the low frequency components agrees with the theory [29]. In conclusion, by optimizing the parameters of the horn-gun the peak electric field can be strongly increased and the pulse shape can be well predicted.

4. Electron acceleration

The simulation of the electron acceleration was carried out by the PIC solver of CST Studio. We assumed that photoelectrons are generated inside the gun structure by the 100 fs long pulses at the fourth harmonic (257 nm) of our 1030 nm wavelength laser. The initial electron bunch is modeled by 6000 macroparticles having 0.1 eV initial mean kinetic energy. The initial velocities are distributed in a hemisphere and the total charge was ~1 fC.

By closing the end of the horn-gun, at the injection point of the electrons an interference is formed between the forward propagating and the reflected pulses. In our simulation of a closed horn-gun structure the peak electric field increases from 500 kV/cm to around 8 MV/cm. The interference of the electric- and magnetic fields affect both the efficiency of the acceleration and the propagation direction of the electron bunch. In the optimized case the electric fields are added together, so the peak electric field is almost doubled, while the magnetic field is almost

Optics EXPRESS

canceled out. This condition ensures efficient acceleration and allows the electrons to propagate perpendicularly to the propagation direction of the THz pulse and not collide with the wall of the channel.

According to our numerical calculations, using 0.55 THz pulse with 500 kV/cm peak electric field at the entrance of the horn-gun – applying the proper synchronization between the photoelectron generating laser and the THz pulse – the mean energy of the electron bunch is increased from rest to ~8 keV with an energy spread of about 6.7% (rms). The evolution of the electron bunch energy along the propagation direction is shown in Fig. 4(a). At the end of the waveguide channel the decrease of the energy is caused by the fact that the central frequency of the THz pulse was higher than originally planned (0.55 THz instead of 0.45 THz). The black dashed line illustrates the end of the waveguide channel in the x direction. Due to the diffraction of the THz pulse at the edge of the exit channel, the electron energy decreases at the vicinity of the exit of the horn-gun. The red dashed line shows the energy evolution of a single electron. The energy and the spatial distribution of the bunch at the exit of the horn-gun is shown in Fig. 4(b) and Fig. 4(c), respectively. The longitudinal size of the bunch is 0.63 ps (FWHM = 33 μm). The normalized emittances of the uncompressed bunch in the x and y direction are $\varepsilon_{n,x} = 6.18$ nm rad and $\varepsilon_{n,y} = 8.10$ nm rad, while deflection angles are $\alpha_x = 2.8°$, $\alpha_y = 0°$. The predicted high-quality electron bunches can be used in the experiments of electron diffraction studies. Applying additional horn-guns as a linear accelerator we could achieve even higher electron energies. Furthermore, we have to note that if the length of the channel is increased to $\lambda/2$ or the channel is opened, the device can be used as a THz-streak camera, too. However, these concepts are beyond our present investigations.

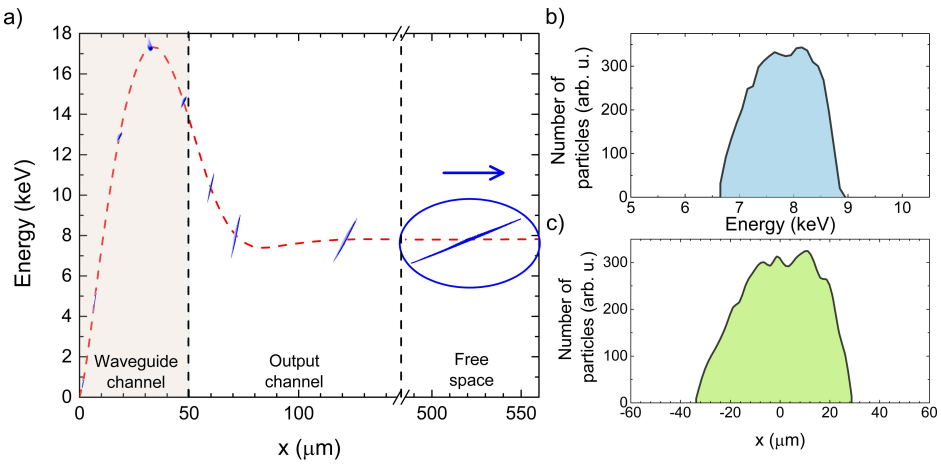

Fig. 4. (a) Energy evolution of the electron bunch along the propagation direction. The phase-space distribution of the electron bunch is indicated at a few positions by blue color. (b) Energy and (c) spatial distribution of the bunch at the exit of the channel.

5. Conclusion

In conclusion, we have numerically investigated the electron bunch acceleration capabilities of a compact setup based on a horn-gun waveguide structure excited by μJ-energy level single-cycle THz pulse. We experimentally measured the waveform of the THz pulse at the exit plane of the opened horn-gun using reflective EOS. The experimental and simulation results agree well, the enhancement of the electric fields corresponds with each other. We theoretically demonstrate

Optics EXPRESS

the acceleration of 1 fC electron bunch from rest up to 8 keV mean energy with 6.7% energy spread (rms). Our calculation shows that using the waveguide structure we can achieve sufficient acceleration gradient for femtocoulomb electron bunches. The predicted ultrashort electron bunches with narrow energy distribution are well suited for ultrafast time resolved electron diffraction studies.

Funding. Emberi Eroforrások Minisztériuma (B-0249); Nemzeti Kutatási Fejlesztési és Innovációs Hivatal (129134, FK-OTKA); Innovációs és Technológiai Minisztérium (2018-1.2.1-NKP-2018-00010).

Acknowledgments. We thank József A. Fülöp for discussions during the initial stage of the horn-gun manufacturing and Sergey Antipov for manufacturing the horn-gun. Gergő Krizsán acknowledges support from the ÚNKP-21-4 New National Excellence Program of the Ministry for Innovation and Technology from the source of the National Research, Development and Innovation Office. Zoltán Tibai would like to thank the support of the János Bolyai Research Scholarship of the Hungarian Academy of Science.

The project has been supported by the National Research, Development and Innovation Office (2018-1.2.1-NKP-2018-00010), the Hungarian Scientific Research Fund (OTKA) (129134), the Ministry of Human Resources (human resource support manager), in the Program of National Talent Program NTP-NFTÖ-21-scholarship (Szabolcs Turnár, B-0249).

Disclosures. The authors declare no conflicts of interest.

Data availability. The data that support the findings of this study are available within the article and from the corresponding author upon reasonable request.

References

1. T. Tajima and J.M. Dawson, "Laser Electron Accelerator," Phys. Rev. Lett. **43**(4), 267–270 (1979).
2. W. Leemans and E. Esarey, "Laser-driven plasma-wave electron accelerators," Phys. Today **62**(3), 44–49 (2009).
3. T. Plettner, P.P. Lu, and R.L. Byer, "Proposed few-optical cycle laser-driven particle accelerator structure," Phys. Rev. Accel. Beams **9**(11), 111301 (2006).
4. E. A. Peralta, K. Soong, R. J. England, E. R. Colby, Z. Wu, B. Montazeri, C. McGuinness, J. McNeur, K. J. Leedle, D. Walz, E. B. Sozer, B. Cowan, B. Schwartz, G. Travish, and R. L. Byer, "Demonstration of electron acceleration in a laser-driven dielectric microstructure," Nature **503**(7474), 91–94 (2013).
5. W. R. Huang, A. Fallahi, X. Wu, H. Cankaya, A.-L. Calendron, K. Ravi, D. Zhang, E. A. Nanni, K.-H. Hong, and Franz X. Kärtner, "Terahertz-driven, all-optical electron gun," Optica **3**(11), 1209–1212 (2016).
6. D. A. Walsh, D. S. Lake, E. W. Snedden, M. J. Cliffe, D. M. Graham, and S. P. Jamison, "Demonstration of sub-luminal propagation of single-cycle terahertz pulses for particle acceleration," Nat. Commun. **8**(1), 421 (2017).
7. P. Salén, M. Basini, S. Bonetti, J. Hebling, M. Krasilnikov, A. Y. Nikitin, G. Shamuilov, Z. Tibai, V. Zhaunerchyk, and V. Goryashko, "Matter manipulation with extreme terahertz light: Progress in the enabling THz technology," Phys. Rep. **836-837**, 1–74 (2019).
8. B. Zhang, Z. Ma, J. Ma, X. Wu, C. Ouyang, D. Kong, T. Hong, X. Wang, P. Yang, L. Chen, Y. Li, and J. Zhang, "1.4-mJ High Energy Terahertz Radiation from Lithium Niobates," Laser Photonics Rev. **15**(3), 2000295 (2021).
9. Gy. Tóth, L. Pálfalvi, Sz. Turnár, Z. Tibai, G. Almási, and J. Hebling, "Performance comparison of lithium-niobate-based extremely high-field single-cycle terahertz sources," Chin. Opt. Lett. **19**(11), 111902 (2021).
10. G. Krizsán, Z. Tibai, J. Hebling, L. Pálfalvi, G. Almási, and Gy. Tóth, "Lithium niobate and lithium tantalate based scalable terahertz pulse sources in reflection geometry," Opt. Express **28**(23), 34320–34327 (2020).
11. M. A. K. Othman, M. C. Hoffmann, M. E. Kozina, X. J. Wang, R. K. Li, and E. A. Nanni, "Parallel-plate waveguides for terahertz-driven MeV electron bunch compression," Opt. Express **27**(17), 23791–23800 (2019).
12. E. C. Snively, M. A. K. Othman, M. Kozina, B. K. Ofori-Okai, S. P. Weathersby, S. Park, X. Shen, X. J. Wang, M. C. Hoffmann, R. K. Li, and E. A. Nanni, "Femtosecond Compression Dynamics and Timing Jitter Suppression in a THz-driven Electron Bunch Compressor," Phys. Rev. Lett. **124**(5), 054801 (2020).
13. L. Zhao, H. Tang, C. Lu, T. Jiang, P. Zhu, L. Hu, W. Song, H. Wang, J. Qiu, C. Jing, S. Antipov, D. Xiang, and J. Zhang, "Femtosecond Relativistic Electron Beam with Reduced Timing Jitter from THz Driven Beam Compression," Phys. Rev. Lett. **124**(5), 054802 (2020).
14. D. Zhang, M. Fakhari, H. Cankaya, A.-L. Calendron, N. H. Matlis, and Franz X. Kärtner, "Cascaded Multicycle Terahertz-Driven Ultrafast Electron Acceleration and Manipulation," Phys. Rev. X **10**(1), 011067 (2020).
15. D. Zhang, A. Fallahi, M. Hemmer, H. Ye, M. Fakhari, Y. Hua, H. Cankaya, A.-L. Calendron, L. E. Zapata, N. H. Matlis, and Franz X. Kärtner, "Femtosecond phase control in high-field terahertz-driven ultrafast electron sources," Optica **6**(7), 872–877 (2019).
16. A. Fallahi, M. Fakhari, A. Yahaghi, M. Arrieta, and Franz X. Kärtner, "Short electron bunch generation using single-cycle ultrafast electron guns," Phys. Rev. Accel. Beams **19**(8), 081302 (2016).
17. A. Fallahi and F. Kärtner, "Design strategies for single-cycle ultrafast electron guns," J. Phys. B: At., Mol. Opt. Phys. **51**(14), 144001 (2018).
18. Sz. Turnár, J. Hebling, J. A. Fülöp, Gy. Tóth, G. Almási, and Z. Tibai, "Design of a THz-driven compact relativistic electron source," Appl. Phys. B **127**(3), 38 (2021).

Optics EXPRESS

19. Ö. Apsimon, G. Burt, R. B. Appleby, R. J. Apsimon, D. M. Graham, and S. P. Jamison, "Six-dimensional phase space preservation in a terahertz-driven multistage dielectric-lined rectangular waveguide accelerator," Phys. Rev. Lett **24**(12), 121303 (2021).
20. H. Xu, L. Yan, Y. Du, W. Huang, Q. Tian, R. Li, Y. Liang, S. Gu, J. Shi, and C. Tang, "Cascaded high-gradient terahertz-driven acceleration of relativistic electron beams," Nat. Photonics **15**(6), 426–430 (2021).
21. H. Tang, L. Zhao, P. Zhu, X. Zou, J. Qi, Y. Cheng, J. Qiu, X. Hu, W. Song, D. Xiang, and J. Zhang, "Stable and Scalable Multistage Terahertz-Driven Particle Accelerator," Phys. Rev. Lett. **127**(7), 074801 (2021).
22. E. Nanni, W. R. Huang, K.-H. Hong, K. Ravi, A. Fallahi, G. Moriena, R. J. D. Miller, and F. X. Kärtner, "Terahertz-driven linear electron acceleration," Nat. Commun. **6**(1), 8486 (2015).
23. M. T. Hibberd, A. L. Healy, D. S. Lake, V. Georgiadis, E. J. H. Smith, O. J. Finlay, T. H. Pacey, J. K. Jones, Y. Saveliev, D. A. Walsh, E. W. Snedden, R. B. Appleby, G. Burt, D. M. Graham, and S. P. Jamison, "Acceleration of relativistic beams using laser-generated terahertz pulses," Nat. Photonics **14**(12), 755–759 (2020).
24. V. Georgiadis, A. L. Healy, M. T. Hibberd, G. Burt, S. P. Jamison, and D. M. Graham, "Dispersion in dielectric-lined waveguides designed for terahertz-driven deflection of electron beams," Appl. Phys. Lett. **118**(14), 144102 (2021).
25. D. Zhang, A. Fallahi, M. Hemmer, X. Wu, M. Fakhari, Y. Hua, H. Cankaya, A.-L. Calendron, L. E. Zapata, N. H. Matlis, and F. X. Kärtner, "Segmented terahertz electron accelerator and manipulator (STEAM)," Nat. Photonics **12**(6), 336–342 (2018).
26. http://www.cst.com
27. M. D. Forno, V. Dolgashev, G. Bowden, C. Clarke, M. Hogan, D. McCormick, A. Novokhatski, B. Spataro, S. Weathersby, and S. G. Tantawi, "rf breakdown tests of mm-wave metallic accelerating structures," Phys. Rev. Accel. Beams **19**(1), 011301 (2016).
28. L. Tokodi, J. Hebling, and L. Pálfalvi, "Optimization of the Tilted-Pulse-Front Terahertz Excitation Setup Containing Telescope," J. Infrared, Millimeter, Terahertz Waves **38**(1), 22–32 (2017).
29. W. C. Chew, "Theory of Microwave and Optical Waveguides," arXiv:2107.09672 (2015).